

# Experimental determination of compressional wave velocities of olivine aggregate up to 1000°C at 1 GPa

Yoshitaka Aizawa<sup>a,1</sup>, Kazuhiko Ito<sup>b</sup>, Yoshiyuki Tatsumi<sup>a,c,\*</sup>

<sup>a</sup>Institute for Geothermal Sciences, Kyoto University, Noguchibaru, Beppu 874-0903, Japan

<sup>b</sup>Faculty of Business Administration, Southern Osaka University, Osaka 587-8555, Japan

<sup>c</sup>Institute for Frontier Research on Earth Evolution (IFREE), Japan Marine Science and Technology Center (JAMSTEC), Yokosuka, 237-0061, Japan

Received 19 April 2000; accepted 28 May 2001

## Abstract

The velocity of the compressional wave ( $V_p$ ) was measured for olivine aggregate at temperatures up to 1000°C at 1 GPa using a piston-cylinder high-pressure apparatus. The samples used in the present study were hot-pressed olivine aggregate with uniform chemical composition. The value of  $V_p$  at 1 GPa and an ambient temperature, is 8.42 km s<sup>-1</sup>, which is identical to that in previous measurements of olivine single-crystals. The temperature derivative of  $V_p$  ( $\partial V_p/\partial T = -4.7 \times 10^{-4}$  km s<sup>-1</sup> K<sup>-1</sup>) obtained from the present experiments at 1 GPa is smaller than the previously reported value at an ambient pressure. The temperature gradient for constant velocity ( $dT/dZ$ )<sub>c</sub> allowing the effect of anelasticity is calculated to be 4°C km<sup>-1</sup>. Taking into account, the temperature gradient in the upper mantle (15°C km<sup>-1</sup> within the lithosphere and 0.6°C km<sup>-1</sup> within the asthenosphere), it is suggested that the low velocity zone in the upper mantle could be caused by a drastic change in the temperature gradient at the lithosphere/asthenosphere boundary. © 2001 Elsevier Science B.V. All rights reserved.

**Keywords:** compressional wave velocity; high pressure; high temperature; olivine aggregate

## 1. Introduction

The elastic wave velocities of inferred mantle constituents determined by laboratory measurements, together with seismic data, provide critical constraints on understanding the structure and compositions of the Earth's mantle (e.g. Duffy and Anderson, 1989; Ita and Stixrude, 1992; Vacher et al., 1998). There has

been a growing interest in obtaining the elastic wave velocity of olivine, because this phase is the major component in the upper mantle (Kumazawa and Anderson, 1969; Niesler and Jackson, 1989; Webb, 1989; Isaak, 1992). However, previous models for the chemical composition of the Earth's mantle have been largely based on experimental data at high pressures and room temperature, or at high temperatures and an ambient pressure. Large extrapolations from such data up to mantle conditions may thus cause serious problems.

The presence of a region of diminished velocity or negative velocity gradient in the upper mantle was first proposed by Gutenberg (1951). The cause of the region is likely to be related to the thermal

\* Corresponding author. Address: Institute for Geothermal Sciences, Kyoto University, Noguchibaru, Beppu 874-0903, Japan. Tel.: +81-977-22-0713; fax: +81-977-22-0965.

<sup>1</sup> Present address: Institute for Study of the Earth's Interior, Okayama University, Misasa, Tottori, 682-0193, Japan.

E-mail address: aizawa@misasa.okayama-u.ac.jp

E-mail address: tatsumi@bep.vgs.kyoto-u.ac.jp (Y. Tatsumi).

boundary between the near surface where, heat is transported by conduction and the deep interior where, heat is transported by convection (Anderson, 1989). Therefore, the experimental data for the temperature derivative of velocity at high pressures is required for the mantle constituents.

Although the pressures obtained are rather low (<1.5 GPa), we have nevertheless developed a method of compressional wave velocity measurement using a piston-cylinder apparatus, because such techniques provide precise velocity data at both elevated pressures and temperatures. In this study, compressional wave velocity ( $V_p$ ) data of olivine aggregates at 1 GPa and up to 1000°C are reported by using a new technique. We further discuss the effect of temperature on  $V_p$  at high pressures and the cause of low velocity zones in the upper mantle.

## 2. Experiments

### 2.1. Starting material

Olivine crystals with 2–3 mm grain size were hand-picked from a spinel lherzolite xenolith from Ichinome-gata, Japan. The chemical composition of the

olivine crystals was analyzed with an electron-probe micro-analyzer (JEOL-JXA8800) at Kyoto University. The forsterite content is constant at Fo<sub>91.6</sub> within a single crystal (Table 1) and almost identical to that of olivine crystals used in the previous studies (e.g. Isaak, 1992). The olivine crystals were ground to ~50 μm grain size in an agate mortar, under acetone. This olivine ‘powder’ was hot-pressed for 2 h at 1 GPa and 1300°C, with a piston-cylinder high-pressure apparatus. The annealed, cylindrical and homogeneous samples (6.0 mm both in diameter and length) obtained in this way were polished and used as starting materials for subsequent experiments. The densities of the samples ( $3.31\text{--}3.34 \times 10^3 \text{ kg m}^{-3}$ ) were calculated based on the cylindrical dimensions and mass.

### 2.2. Velocity measurements

The velocity measurements were carried out using a piston-cylinder apparatus with a 24 mm inner diameter and 80 mm thickness, at Kyoto University. The assembly is shown in Fig. 1. Talc was used as the pressure-transmitting medium. Nickel tubes (23 mm length) were placed at the top and the bottom of a carbon heater (20 mm length) embedded in the center

Table 1  
Chemical composition of olivine

SiO <sub>2</sub>	41.03
TiO <sub>2</sub>	0.00
Al <sub>2</sub> O <sub>3</sub>	0.01
FeO	8.20
MgO	50.28
CaO	0.09
Na <sub>2</sub> O	0.00
K <sub>2</sub> O	0.02
Total	99.63
Oxygen	4.000
Si	1.001
Ti	0
Al	0
Fe	0.167
Mg	1.828
Ca	0.002
Na	0
K	0
Cation sum	2.998
Mg/(Mg + Fe)	0.916

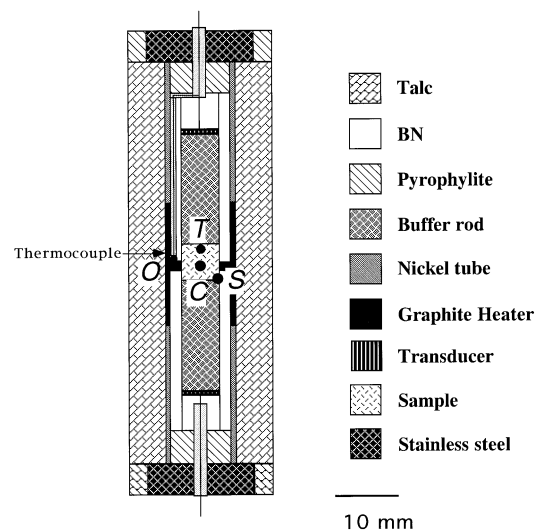


Fig. 1. Schematic representation of the sample assembly for the high pressure chamber. O represents the measurement point of the temperature by thermocouple; C, T and S reveal the points for showing the temperature differences between O and C, O and T and O and S.

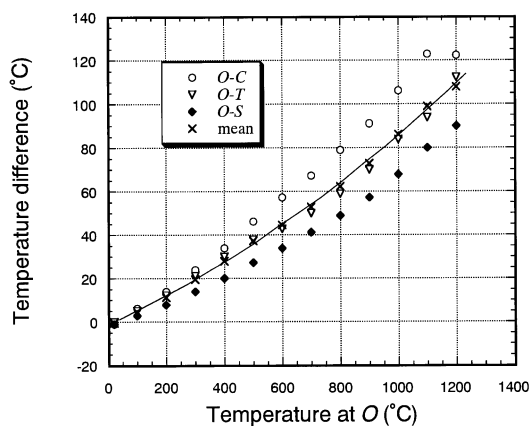


Fig. 2. Temperature differences between O–C (center), O–T (top) and O–S (corner) with temperature.

of the talc, to lower temperatures around the transducers. Pressure was calibrated against the load by using the ultrasonic measurement of the  $\alpha$ – $\beta$  transition of quartz single crystal at 1 GPa and 825°C (Groos and Heege, 1973), assuming that the transition temperature is indicated by the minimum velocity (Kern, 1979). The accuracy of the sample pressure is estimated to be less than  $\pm 0.04$  GPa.  $\text{LiNbO}_3$  transducers (0.5 mm thick,  $36^\circ$  Y-cut) were used to emit and receive the acoustic signals. Each transducer was mounted on the end of a platinum buffer rod. The sample was placed between two platinum (Pt) buffer rods (6.0 mm diameter, 18 mm length) and then wrapped in Pt foil, to avoid direct contact between the sample and the BN (boron nitride) sleeves. No bond material was used at the sample–buffer rod interface to minimize the uncertainty resulting from the thickness of the bond. We used the Pt rods for the buffers because the reflection readily occurs at the sample–buffer rod interface, as a result of the substantial difference in the acoustic impedance. The pulse applied to the transducer generates an elastic wave. We observed the ultrasonic echoes from both transmitted and reflected components. Reflection takes place at the interface between the sample and the second buffer rod, and then, between the sample and the first buffer rod. Travel times were determined from the differences of arrival times between these echoes, as described later.

Temperature was measured by a Chromel/Alumel thermocouple which was not directly in contact with the sample, but was placed at the side (O) of the sample as shown in Fig. 1. Therefore, the temperature differences between O and the insides (C: the center, T: the top, S: the corner) of the sample must be considered. The temperature differences between O and C, between O and T and between O and S were measured from room temperature up to 1200°C at 0.5 GPa and are shown in Fig. 2. The approximate temperature differences at O from the mean temperature of the sample were modified by the solid curve in Fig. 2.

Fig. 3 shows the method of precisely measuring the travel time in the sample. In the pulse transmission technique, it is possible to perform experiments under high temperature by using buffer rods with sufficient length, which can keep the transducers at relatively low temperature. If both echoes through Path I and Path II in Fig. 3 can be observed simultaneously, the travel time ( $2T$ ) for twice the length of the sample ( $2L$ ) can be obtained directly from the difference between travel times through Path I and through Path II. Therefore, the elastic wave velocity in the sample can be obtained from the expression of  $2L/2T$ . The uncertainty of the velocity measurements is better than 1%. The temperature gradient across the sample was estimated to be  $\sim 30^\circ\text{C}$  at 1000°C.

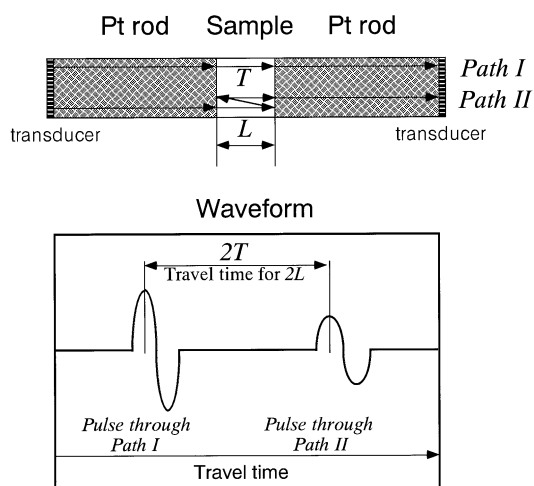


Fig. 3. Schematic representation of the measurement method for determining travel times in the sample.

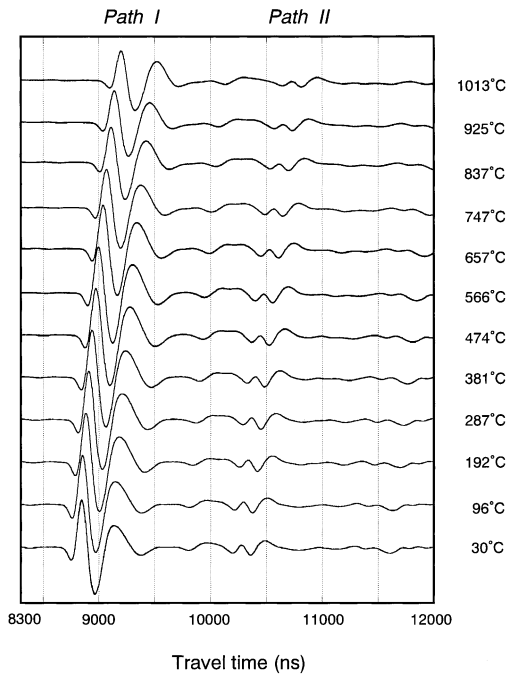


Fig. 4. Temperature variation of the observed waveforms of olivine aggregate up to 1013°C at 1 GPa.

### 3. Results

Fig. 4 shows the temperature variation of the waveforms observed in the present experiments and indicates that the present  $V_p$  measurements are valid at high temperatures, up to 1000°C. The travel times were corrected through the procedure described by

Table 2  
Compressional wave velocity and thermal expansion of olivine

Temp. (°C)	$\alpha$ ( $10^{-5} \text{ K}^{-1}$ )	$V_p$ ( $\text{km s}^{-1}$ )
30	2.60	8.43
96	2.91	8.40
192	3.13	8.36
287	3.27	8.35
381	3.39	8.31
474	3.49	8.26
566	3.58	8.18
657	3.66	8.16
747	3.74	8.13
837	3.81	8.08
925	3.89	8.03
1013	3.96	7.94

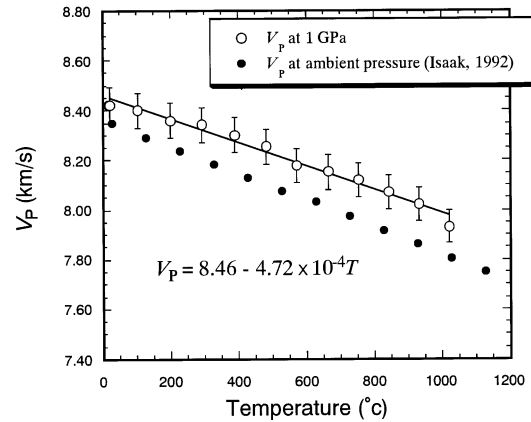


Fig. 5.  $V_p$  as a function of temperature at 1 GPa obtained from this study, together with previous measurements of a single crystal at an ambient pressure [Isaak, 1992].

Niesler and Jackson (1989). The sample length  $L$  at high temperature  $T$  and pressure  $P$  is related to its value at  $L_0$  at zero pressure and  $T_0 = 300 \text{ K}$  by the expression

$$\frac{L_0}{L} = \left[ 1 - \alpha(T - T_0) + \frac{P}{K} \right]^{1/3} \quad (1)$$

where  $\alpha$  and  $K$ , are the thermal expansivity and bulk modulus, respectively. The correction was made for elastic deformation by using a pressure-dependent bulk modulus from Webb (1989), and for thermal expansion using the data of Suzuki (1975). The velocities calculated from the corrected travel times and  $\alpha$  are listed in Table 2 and plotted in Fig. 5 as a function of temperature, together with the results at ambient pressure (Isaak, 1992). The present result at 1 GPa and an ambient temperature ( $8.42 \text{ km s}^{-1}$ ) under conditions identical to the present experiments shows good agreement with those obtained for single crystals ( $8.44\text{--}8.46 \text{ km s}^{-1}$ ). Thus, it may be suggested that, the porosity in the present ‘hot-pressed’ olivine polycrystal is small, although the volumes of the samples are too small to directly measure the porosity. Niesler and Jackson (1989) investigated the velocity–porosity relations of olivine polycrystals at ambient temperature up to 3 GPa and confirmed a negative correlation between velocity and porosity. The present result at an ambient temperature ( $8.42 \text{ km s}^{-1}$ ) is larger than that of their result

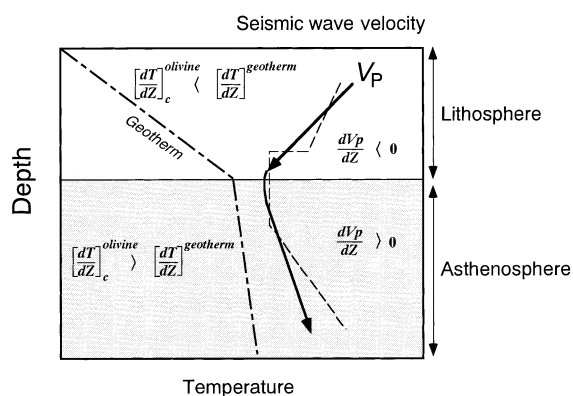


Fig. 6. Relationship between a geotherm estimated by the plate model [McKenzie, 1967] and seismic wave velocity of olivine (upper mantle) as a function of depth. According to the temperature gradient,  $(dV_p/dZ)$  may change from negative to positive at the lithosphere/asthenosphere boundary, causing a low velocity zone. Seismic studies determine the average velocities of the lithosphere and the asthenosphere (dashed line), although the real velocity may change continuously.

( $8.35 \text{ km s}^{-1}$ ) with 0.3% porosity, suggesting that the porosity of the sample is estimated to be less than 0.3%.

The velocities decrease linearly with increasing temperature (Fig. 5). The temperature derivative of  $V_p$  ( $\partial V_p/\partial T = -4.7 \times 10^{-4} \text{ km s}^{-1} \text{ K}^{-1}$ ) calculated based on the present results is lower than that obtained at ambient pressure ( $-5.4 \times 10^{-4} \text{ km s}^{-1} \text{ K}^{-1}$ ) (Isaak, 1992). Ramanantoandro and Manghnani (1978) reported velocities of a dunite (98% olivine), obtained up to  $500^\circ\text{C}$  at 1 GPa. Although their results of  $\partial V_p/\partial T$  were variable ( $-6.7$  to  $-5.4 \times 10^{-4} \text{ km s}^{-1} \text{ K}^{-1}$ ), the mean value for the dunite ( $-6.1 \times 10^{-4} \text{ km s}^{-1} \text{ K}^{-1}$ ) is substantially higher than that of the present value. The difference might be attributed to the presence of minor phases such as orthopyroxene or spinel in the dunite sample.

#### 4. Discussion and conclusions

In order to apply the present results to the seismic profiles of the upper mantle, we adopt the geotherm in a plate model (McKenzie, 1967). Although the geotherm depends on the age of the lithosphere, the temperature gradients are almost constant in older ( $>30 \text{ my.}$ ) lithosphere. The temperature gradient in

the lithosphere is then estimated to be about  $15^\circ\text{C km}^{-1}$  which is identical to the value used in Karato and Jung (1998). Assuming an appropriate thickness of lithosphere, the temperature gradients change abruptly at the lithosphere/asthenosphere boundary. The temperature gradient beneath the lithosphere ( $0.6^\circ\text{C km}^{-1}$ ) is obtained based on the model of McKenzie and Bickle (1988).

The thermal gradient for constant velocity is given by Christensen (1979)

$$\left(\frac{dT}{dZ}\right)_c = \rho g \left[ -\frac{(\partial V_p/\partial P)_T}{(\partial V_p/\partial T)_P} \right] \quad (2)$$

where  $Z$  is depth,  $\rho$  the density and  $g$  is the acceleration due to gravity. Based on  $(\partial V_p/\partial P)_T$  calculated by using the data of Webb (1989) and  $(\partial V_p/\partial T)_P$  obtained in this study, a thermal gradient of  $9^\circ\text{C km}^{-1}$  is calculated for olivine. The temperature dependence of  $V_p$  obtained using a high frequency (6 MHz) in this study is mostly due to anharmonic effect. However, most of the seismological observations are made at low frequencies ( $<1 \text{ Hz}$ ) and contributions from anelastic effects become important (Jackson et al., 1992; Kanamori and Anderson, 1977; Karato, 1993). The temperature derivative allowing anelastic effects is expressed by the following relations (Karato, 1993),

$$\partial \ln V/\partial T \cong \partial \ln V_0/\partial T - (Q^{-1}(\omega, T)/\pi)(H^*/RT^2) \quad (3)$$

where  $V_0$  is seismic wave velocity where only the anharmonic effect is important,  $Q^{-1}(=100)$  is seismic wave attenuation at temperature  $T$  ( $=1600 \text{ K}$ ) and frequency  $\omega$ ,  $H^*$  is the activation enthalpy ( $=500 \text{ kJ mol}^{-1}$ ) (Karato, 1993). Then, we modify the Eq. (2) as

$$\left(\frac{dT}{dZ}\right)_c \cong \rho g \left[ -\frac{(\partial \ln V_p/\partial P)_T}{(\partial \ln V_p/\partial T)_P} \right]. \quad (4)$$

The calculated thermal gradient for constant velocity obtained from the Eq. (4) is  $4^\circ\text{C km}^{-1}$ . We assume the mono-mineralic upper mantle composed only by olivine, simply because of the well-constrained elastic properties and large fraction of olivine ( $>50\%$ ) in the upper mantle. As shown in Fig. 6, the temperature gradient within the lithosphere is greater than the olivine thermal gradient at constant velocity, causing the decrease in the velocity with depth in this region. In contrast, because the

temperature gradient decreases significantly within the asthenosphere, the velocity increases with depth. Although the actual velocity structure may change gradually (Sato et al., 1989), seismic studies resolve only average velocities at average depths of lithosphere and asthenosphere. The present results experimentally support the model in which an abrupt change of the thermal gradient is likely to be a possible cause for the low velocity zones in the upper mantle.

### Acknowledgements

We are grateful to Drs T. Kawamoto, I. Kushiro and S. Yamashita for their helpful suggestions in sample preparations.

### References

- Anderson, D.L., 1989. *Theory of the Earth*. Blackwell, Cambridge 366 pp.
- Christensen, N.I., 1979. Compressional wave velocity in rocks at high temperatures and pressures, critical thermal gradients, and crustal low velocity zones. *J. Geophys. Res.* 80, 6849–6857.
- Duffy, T.S., Anderson, D.L., 1989. Seismic velocities in mantle minerals and the mineralogy of the upper mantle. *J. Geophys. Res.* 94, 1895–1912.
- Groos, A.F., Heege, J.P., 1973. The high–low quartz transition up to 10 kbars pressure. *J. Geol.* 81, 717–724.
- Gutenberg, B., 1951. Crustal layers of the continents and oceans. *Geol. Soc. Am. Bull.* 62, 427–440.
- Isaak, D.G., 1992. High temperature elasticity of iron-bearing olivines. *J. Geophys. Res.* 97, 1871–1885.
- Ita, J., Stixrude, L., 1992. Petrology, elasticity and composition of the mantle transition zone. *J. Geophys. Res.* 97, 6849–6866.
- Jackson, I., Paterson, M.S., Fitz Gerald, J.D., 1992. Seismic wave dispersion and attenuation in Åheim dunite. *Geophys. J. Int.* 108, 517–534.
- Kanamori, H., Anderson, D.L., 1977. Importance of physical dispersion in surface-wave and free-oscillation problems, review. *Rev. Geophys. Space Phys.* 15, 105–112.
- Karato, S-I., 1993. Importance of anelasticity in the interpretation of seismic tomography. *Geophys. Res. Lett.* 20, 1623–1626.
- Karato, S-I., Jung, H., 1998. Water, partial melting and the origin of the seismic low velocity and high attenuation zone in the upper mantle. *Earth Planet. Sci. Lett.* 157, 193–207.
- Kern, H., 1979. Effects of high–low quartz transition on compressional and shear wave velocities in rocks under high pressure. *Phys. Chem. Miner.* 4, 161–171.
- Kumazawa, M., Anderson, O.L., 1969. Elastic moduli, pressure derivatives and temperature derivatives of single-crystal olivine and single crystal forsterite. *J. Geophys. Res.* 74, 5961–5972.
- McKenzie, D.P., 1967. Some remarks on heat flow and gravity anomalies. *J. Geophys. Res.* 72, 6261–6271.
- McKenzie, D., Bickle, M.J., 1988. The volume and composition of melt generated by extension of the lithosphere. *J. Petrol.* 29, 625–679.
- Niesler, H., Jackson, I., 1989. Pressure derivatives of elastic wave velocities from ultrasonic interferometric measurements on jacketed polycrystals. *J. Acoust. Soc. Am.* 86, 1573–1585.
- Ramanantoandro, R., Manghnani, M.H., 1978. Temperature dependence of the compressional wave velocity in isotropic dunite: measures to 500°C at 10 kbar. *Tectonophysics* 47, 73–84.
- Sato, H., Sacks, I.S., Murase, T., 1989. The use of laboratory velocity data for estimating temperature and partial melt fraction in the low-velocity zone: Comparison with heat flow and electrical conductivity studies. *J. Geophys. Res.* 94, 5689–5704.
- Suzuki, I., 1975. Thermal expansion of periclase and olivine, and their anharmonic properties. *J. Phys. Earth* 23, 145–159.
- Vacher, P., Mocquet, A., Sotin, C., 1998. Computation of seismic profiles from mineral physics: the importance of the non-olivine components for explaining the 660 km depth discontinuity. *Phys. Earth Planet. Int.* 106, 275–298.
- Webb, S.L., 1989. The elasticity of the upper mantle orthosilicates olivine and garnet to 3 GPa. *Phys. Chem. Miner.* 16, 684–692.